P170526

Hydrological Modelling Report

Assessment of Suitable Flood Mitigation Measures (based on Dukniskhevi River Extreme Flood Analysis) in Tbilisi, Georgia

CTCN REFERENCE NUMBER: 2016000043

Document Information

Date	23.04.2018
HYDROC project no.	P170526
HYDROC responsible	Juan Fernandez
Client	CTC-N/UNIDO
Reference No.	2016000043
Project No.	
Credit No.	

Contact
HYDROC GmbH
Siegum 4
24960 Siegum
Germany

Tel - +49 172 450 91 49
Email - info@hydroc.de

Table of Contents

List of Abbreviations

DEM	Digital Elevation Model
GIS	Geographical Information System
HEC-DSS	Hydrologic Engineering Center – Data Storage System
HEC-HMS	Hydrologic Engineering Center – Hydrologic Modelling System
HEC-RAS	Hydrologic Engineering Center – River Analysis System
Ks	Saturated hydraulic conductivity
NEA	National Environment Agency
PET	Potential Evapotranspiration
R	Storage coefficient of the Clark Transform Method
RP	Return Period
Tc	Time of concentration
SCS-CN	Soil Conservation Service – Curve Number
USACE	United States Army Corps of Engineers

1 Introduction

The 24km²-catchment area of the ungauged river Leghvtakhevi is subject to a complex hydrological setting. The river catchment is very steep, and precipitation is characterized by intense orographic rainfall events. Due to this, the river can cause strong flash floods. Flash floods, as a result of heavy rains have hit Tbilisi in the recent past, causing heavy damages or even catastrophes. Against this background, the activities of the overall project represent intensive work on a single river catchment including hydrological modelling, climate change impact assessment, hydraulic modelling, flood mapping, proposal for flood mitigation and adaptation measures.

This hydrological report describes the available data, the hydrologic model setup, model parameterization, results and related uncertainties from the simulations of current and future climate change conditions. The main challenge of the model application in the Leghvtakhevi is the extremely short response time of the catchment and the lack of appropriate hydro-climatic data in sufficient length and temporal resolution. In the neighbouring catchment of the Leghvtakhevi, the Vere, daily discharge data exists, which is the only option to carry out a basic calibration of the Leghvtakhevi model through a parameter transfer. Therefore, two hydrologic models are setup within the scope of this project.

An important aspect of the project is the technology and knowledge transfer to the National Environmental Agency (NEA) and relevant stakeholders, handing over software and models as well as providing thorough training and capacity building to enable stakeholders to fully benefit and make use of the developed technologies.

2 Catchment Description

The Leghvtakhevi catchment is located in the western part of Tbilisi. The catchment area is 24km² and has a high topographic gradient, ranging from about 1440 to 390mASL along a West-East slope of less than 10km in length (Figure 1). The Vere catchment is the neighbouring catchment, located directly north. The Vere has an area of about 175km², but shows a comparable topography, land use and soil distribution. Main focus in this study lies on the ungauged Leghvtakhevi catchment, but because discharge data is available in the Vere catchment, it is considered in the hydrologic model for basic parameter estimation and their transfer to the Leghvtakhevi model.

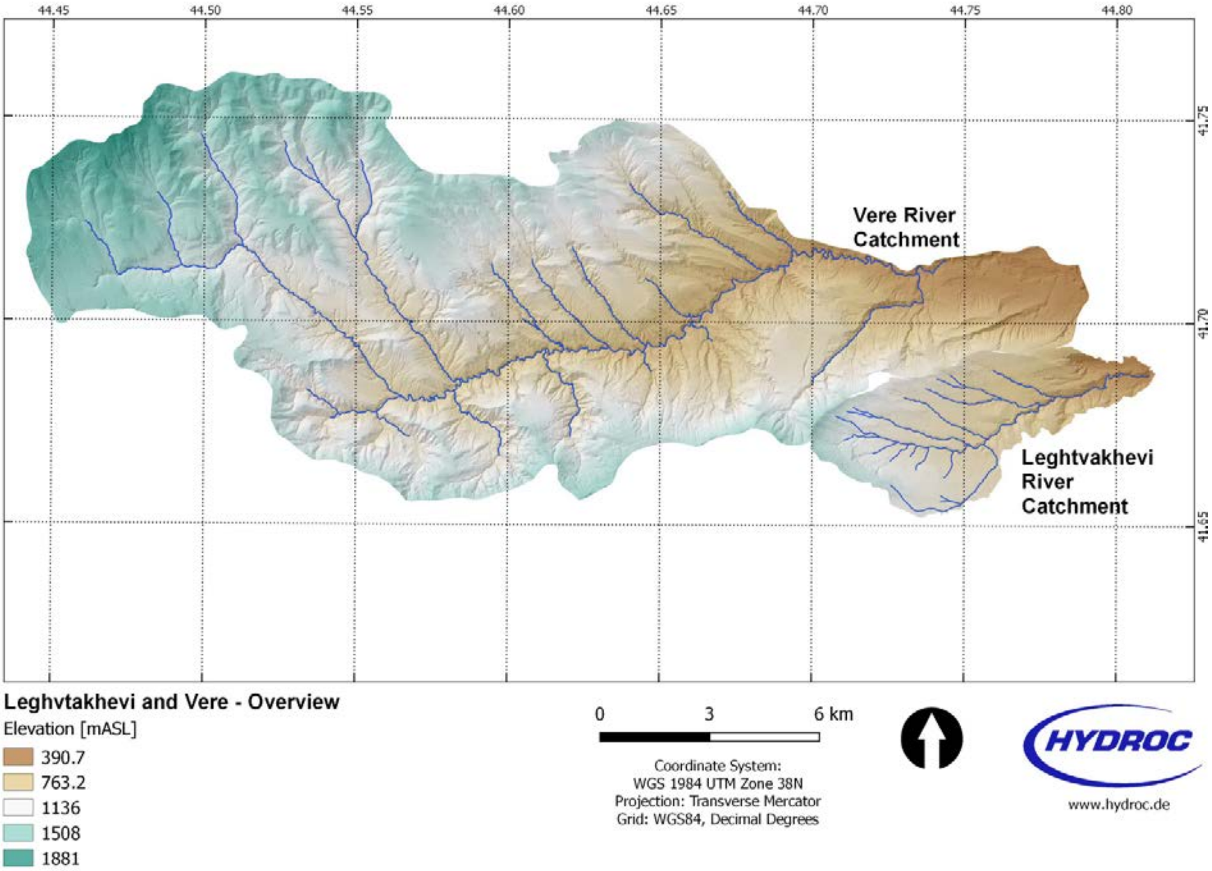

Figure 1 – Topography and stream network of the Leghvtakhevi and Vere River catchments

In both catchments, high elevations of more than 1200mASL are covered by light forests and shrub land (Figure 1a), while the remaining areas are mainly arable land and covered by urban areas (Figure 1b). In the lower part, the Leghvtakhevi flows in an accessible gorge (Figure 1c), surrounded by rock outcrops, bare soils, shrub land and trees (Figure 1d). Soil types are alternating between thick and shallow brown forest soils, thick and shallow heavy loam and clayey loam, indicating a very high runoff potential. Both rivers discharge into the Kura (Mtkvari) river near the centre of Tbilisi.

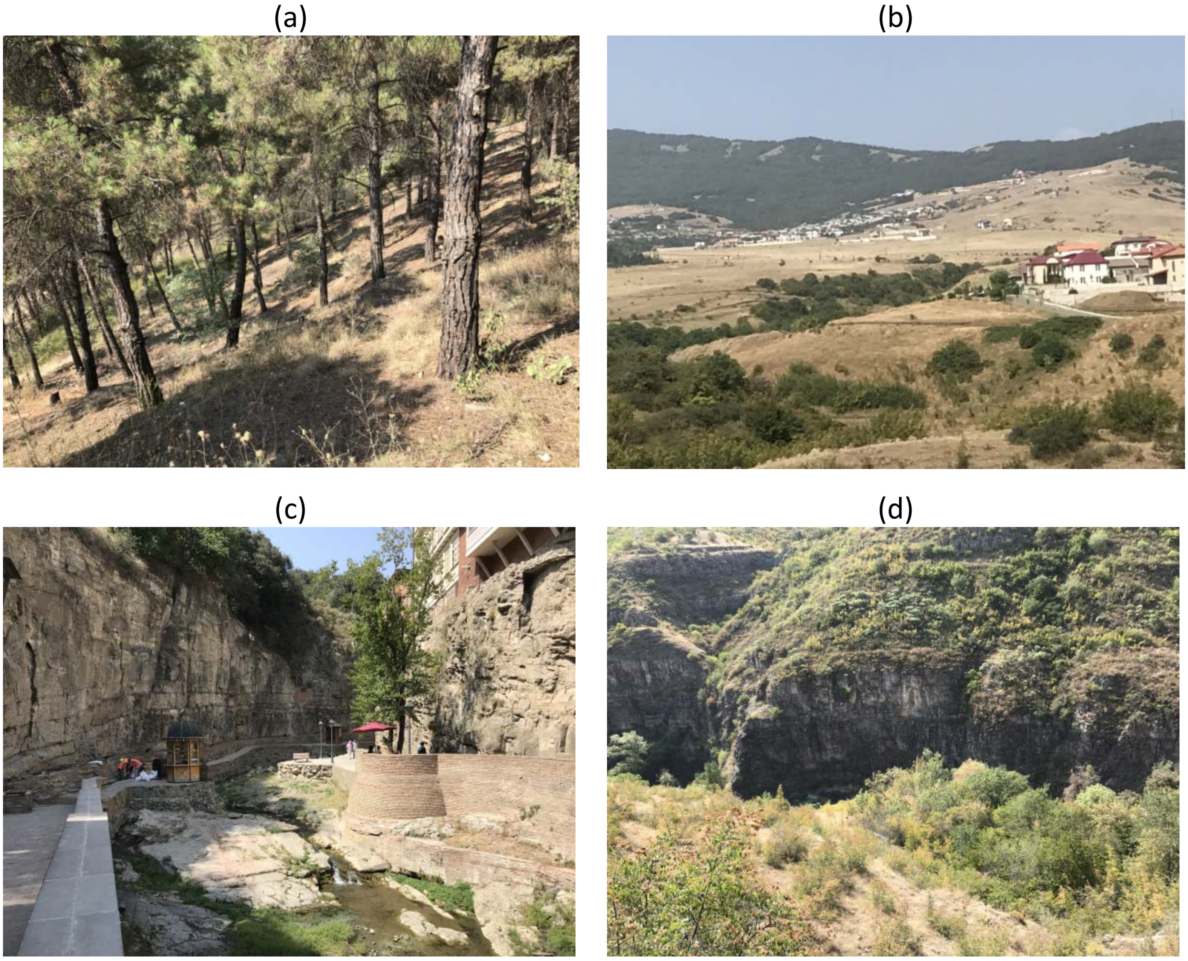

Figure 2 – Impressions of the catchment area (a) forests, (b) arable land and settlements in the central part, (c) the gorge incised by the Leghvtakhevi River in the lower part as viewed from the bottom and (d) from the top

3 Data collection, analysis and processing

The following data (Table 1) have been collected and assessed for both the Leghvtakhevi catchment and the neighbouring Vere catchment:

Table 1 – Overview of data sources used for the hydrological model

Description	Resolution	Source	Year
Digital Elevation Model	1m	Supplied by NEA	unknown
Stream network	Polygon (original resolution unknown)	Supplied by NEA	unknown
Discharge locations for hydraulic model	Point data	Derived within project	2018
Land use map	Polygon (original resolution unknown)	Supplied by NEA	unknown
Google Earth images	Around 1-10m	Google Earth	2017
Soil map and soil texture	Polygon, 1:200000	Supplied by NEA	unknown
Daily precipitation data	Gauges Kojori, Tbilisi Airport, Vashlijvari	Supplied by NEA	Data ends in 2016
Radar precipitation observations	3min temporal for four storm events	Supplied by NEA	2016
Daily discharge data of the Vere river	1 day	Supplied by NEA	Data ends in 2015

3.1 Topography and stream network data

Topographic data is required to derive the catchment boundaries, discretise the catchment in suitable sub-basins, derive the stream network and calculate overland and channel slopes. This information is essential for calculating the amount of water and time it requires to translate rainfall to the flood-wave in the channel at the points of interest. The available 1m digital elevation model (DEM) provides a sufficient resolution and quality for that task.

The supplied stream network was evaluated and checked regarding the overlay with the DEM and Google Earth and will be used during the model setup process to force the delineation of streams to the correct locations.

In close consultation with the hydraulic modelling expert, suitable points were agreed in the Leghvtakhevi where discharge data needs to be passed on to the hydraulic model. At these locations, additional sub-basin outlets need to be defined in the hydrologic model.

3.2 Soil data, land use data and saturated hydraulic conductivity

Land cover data is required to derive surface roughness for calculating overland flow velocities, initial losses of rainfall (interception) and runoff coefficients for infiltration rates (e.g. impermeable areas). The supplied land cover data distinguishes eight classes. Using satellite images, it was reclassified according to its major hydrological properties.

Table 2 – Reclassification of Land use and assigning impervious area ratios

Original	Reclassified	Impervious Area [%]
CEMETARY	Light Forest	0
FOREST_LITE	Light Forest	0
GROUND	Light Forest	0
LAND	Arable / Shrubland	0
LARGE_CITY	Urban high density	60
LARGE_RIVER	Water	100
ROCKY	Rock outcrops	90
SCRUB	Shrub land	0
SMALL_CITY	Urban low density	40
URBAN_PARK	Shrub land	0
LAKE	Water	100
ORCHARD	Light Forest	0

Information on soil type distribution and soil properties are important data to derive infiltration values into the soil. The supplied soil maps contain information on the hydrologic soil group and soil texture

An overview of the derived spatial datasets for the Leghvtakhevi is given in Figure 3. The same datasets, apart from the discharge points for the hydraulic model were processed for the Vere too.

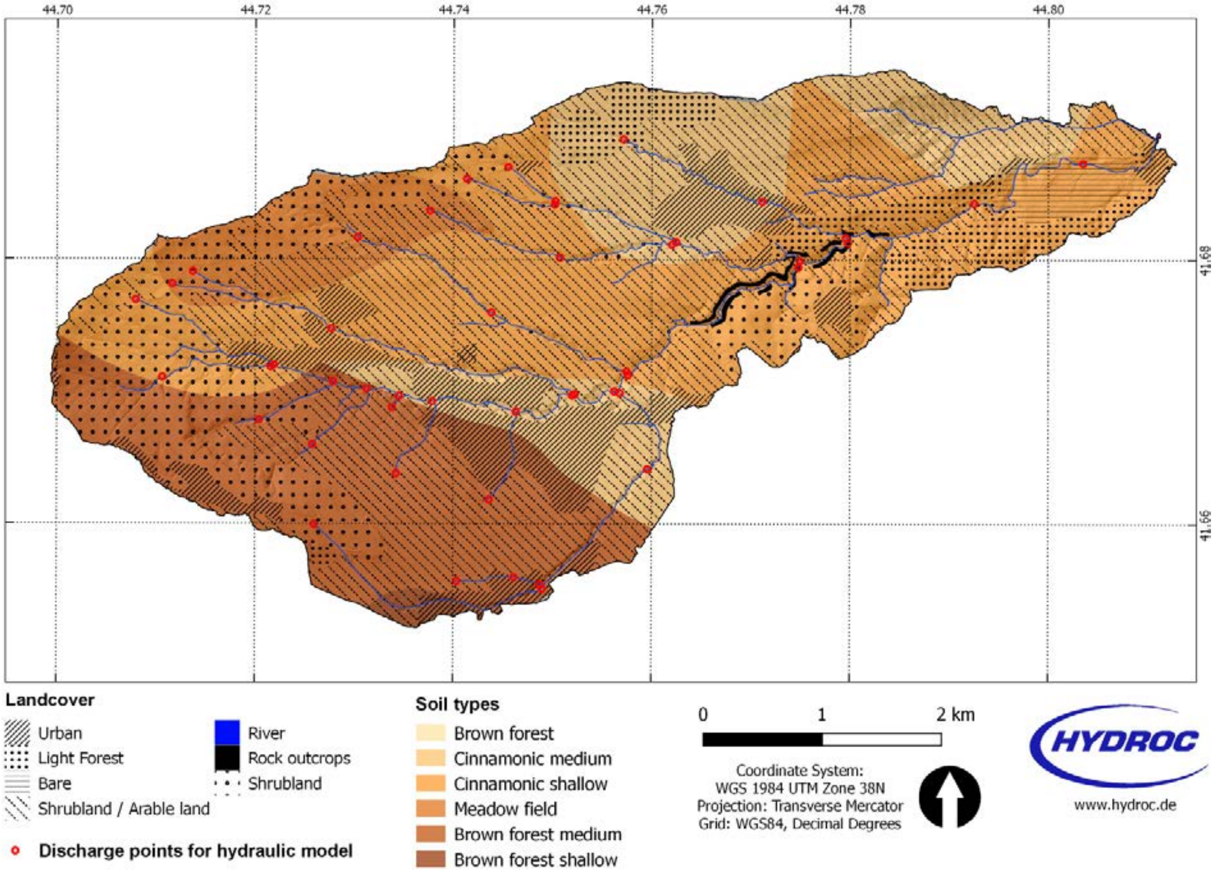

Figure 3 – Spatial data overview of hill-shaded 1m DEM, soil types, land use with stream network and the discharge points for the hydraulic model

3.3 Daily precipitation data processing

The most important input data for the hydrologic simulations of individual flood events is appropriate rainfall data. Due to the relatively small catchment size and high slopes, the response time of the Leghvtakhevi catchment is in the range of 1hour according to calculations using the USACE “TR-55” method, while the response time of the Vere lies in the range of 5.4hours. Individual sub-basins will therefore have response times in the range of minutes. This makes sub-hourly simulation time steps necessary in both catchments in order to being able to sufficiently capture and resolve the flood peak including rising and falling limb of the hydrograph.

However, only daily precipitation data from the three stations Vashlijvari, Tbilisi Airport and Kojori could be supplied by NEA (Table 3, Figure 4). Data were analysed for gaps. Gaps of 1 day were filled through linear interpolation of the previous and next day, and gaps larger than 1 day were filled by the neighbouring station.

Table 3 – Precipitation gauges, location, elevation and data availability

Station	Lat	Long	Elevation	Begin year	End year
Vashlijvari	41.75785	44.75518	427	1961	2016
Tbilisi Airport	41.66834	44.95577	462	1980	2010
Kojori	41.66018	44.69906	1381	1961	2005

Observations of the closest gauge to both catchments, Kojori, unfortunately stopped in 2005, but the extrapolation of the Kojori time series to 2016 is needed for the temporal downscaling of the daily data to a subdaily time step. Since 2016, a precipitation radar station is operating in the region and is the only option to obtain subdaily storm distributions for the Leghvtakhevi. To extent the daily time of Kojori, an analysis of the overlapping data between the stations was carried out with the following results:

- Vashlijvari vs Tbilisi Airport: r = 0.62
- Vashlijvari vs Kojori: r = 0.73
- Tbilisi Airport vs Kojori = 0.57

This indicates, that the data of Vishlijvari is most suitable to extent the Kojori time series up to the year 2016. This extension was carried out using distribution (or quantile) mapping. This method compares the long-term frequency distributions of the daily source data (Vishlijvari) and the daily target data (Kojori) for each month of the year. The difference between the frequency distributions are expressed as monthly parameters that are used to translate the

Vishlijvari frequency distributions after 2005 to Kojori. The distribution mapping is superior to more simple methods (e.g. linear regression) since it performs best in depicting averages, standard deviations and maximum values.

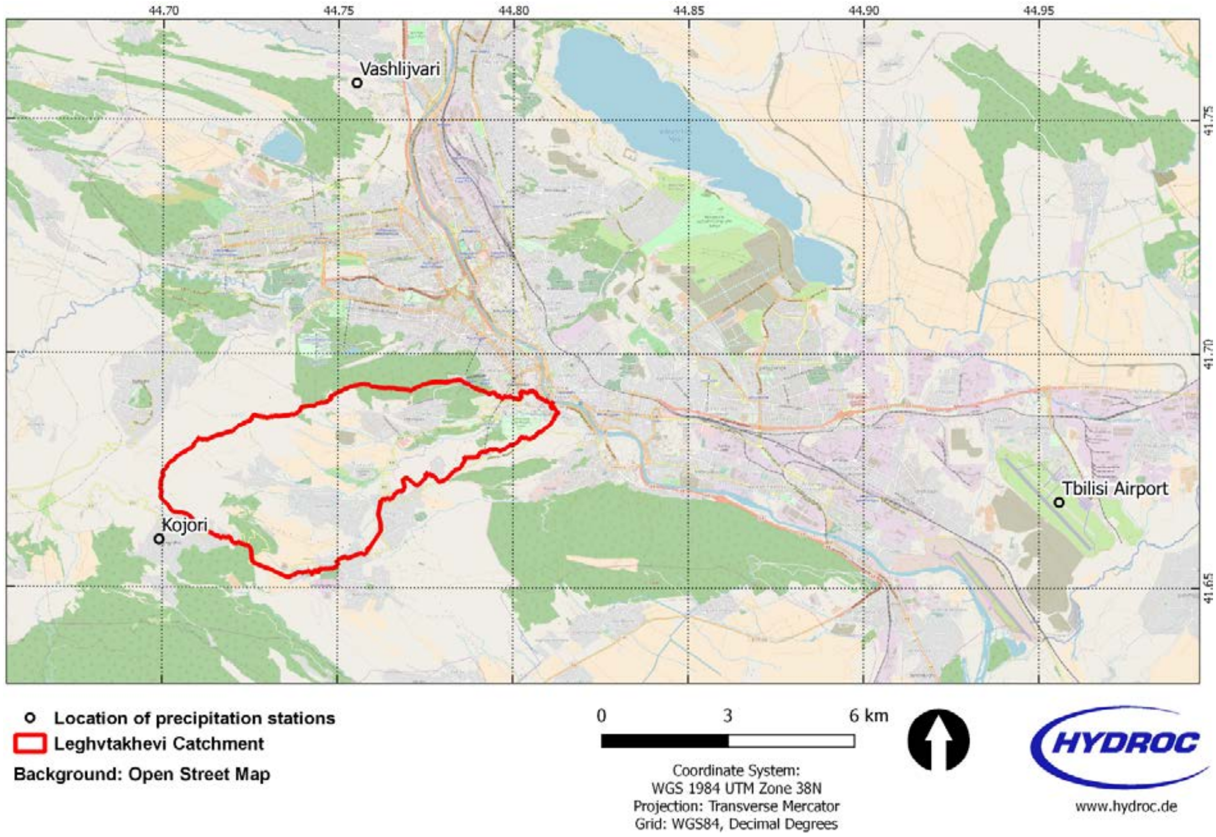

Figure 4 – Location of the Leghvtakhevi catchment and closest precipitation stations (for data availability of stations, see Table 3)

3.4 Radar precipitation data processing

The overlap period between the extrapolated precipitation data at Kojori and the radar station data is the year 2016. For this time period, the highest daily precipitation intensities in 2016 were selected and radar data was acquired (Table 4). The radar data for the selected events (10GB) was supplied by Delta (a public company within the Ministry of Defence of Georgia) the binary 'Rainbow®[1]' data format. The open source Library for Weather Radar Data Processing (WRADLIB)[2] is available to read the data. In order to use precipitation radar data for hydrologic modelling and to obtain the precipitation height as shown in Table 4, a number of processing steps were implemented in a Python script:

(1) The location of the radar station was extracted, which is located about 100km east of the Leghvtakhevi catchment (Figure 5). The elevation profile between the radar station location and the Leghvtakhevi catchment (Figure 5) shows that no mountains impede the radar beam.

(2) A decision has to be made about the radar beam inclination to be used: The radar data is observed in three-minute intervals, in ten inclinations (=slices from about 0 to 40°) of the radar beam for each interval. As can be seen in Figure 6, the higher the inclination, the less reflectivity (dBZ) is observed in the outer regions. In these cases, the radar beam's height passes the upper clouds. Therefore, to obtain precipitation estimates further away from the radar station, it is required to use the lowest inclinations. However, even for an angle of 0° (Slice 0, which is used in this study), Earth's curvature and the distance from the radar station to the Leghvtakhevi (100km) leads to rainfall observations in 785m[3] height above the radar station.

(3) Erroneous reflectivity values can be caused by non-rainfall objects. The clutter filter by Gabella et al. (2002)[4] is used to remove clutter within each extracted slice and each time step.

(4) Reflectivity values then need to be converted to precipitation rate. Therefore, the following equations are applied:

$$Z_{nat} = 10^{\frac{Z}{10}}$$

where Z_{nat} is the reflectivity in natural units (mm^6 / mm^3) and Z is the reflectivity in dBZ, and

$$R = \left(\frac{Z_{nat}}{200}\right)^{\frac{1}{1.6}}$$

---

[1] http://www.de.selex-es.com/capabilities/meteorology/products/components/rainbow5

[2] http://wradlib.org/

[3] http://earthcurvature.com/

[4] Marco Gabella and Riccardo Notarpietro. Ground clutter characterization and elimination in mountainous terrain. In *Use of radar observations in hydrological and NWP models*, 305–311. Katlenburg-Lindau, 2002. Copernicus. URL: http://porto.polito.it/1411995/.

where R is the rainfall intensity in mm/hr.

Table 4 – Selected storm events in 2016 of the extrapolated Kojori gauge and the radar data

Date	Kojori gage	Radar Slice 0	Notes
	mm/d		
07.06.2016	18.3	48.2	
08.06.2016	3.4	4.0	
09.06.2016	12.0	56.2	
10.06.2016	18.6	18.4	
01.07.2016	32.8	1.0	Radar data not complete
21.09.2016	9.8	16.9	
22.09.2016	0.0	10.6	
23.09.2016	51.4	45.9	
24.09.2016	6.6	4.7	
16.11.2016	5.0	33.6	Major rainfall occurred around midnight
17.11.2016	35.1	21.5	

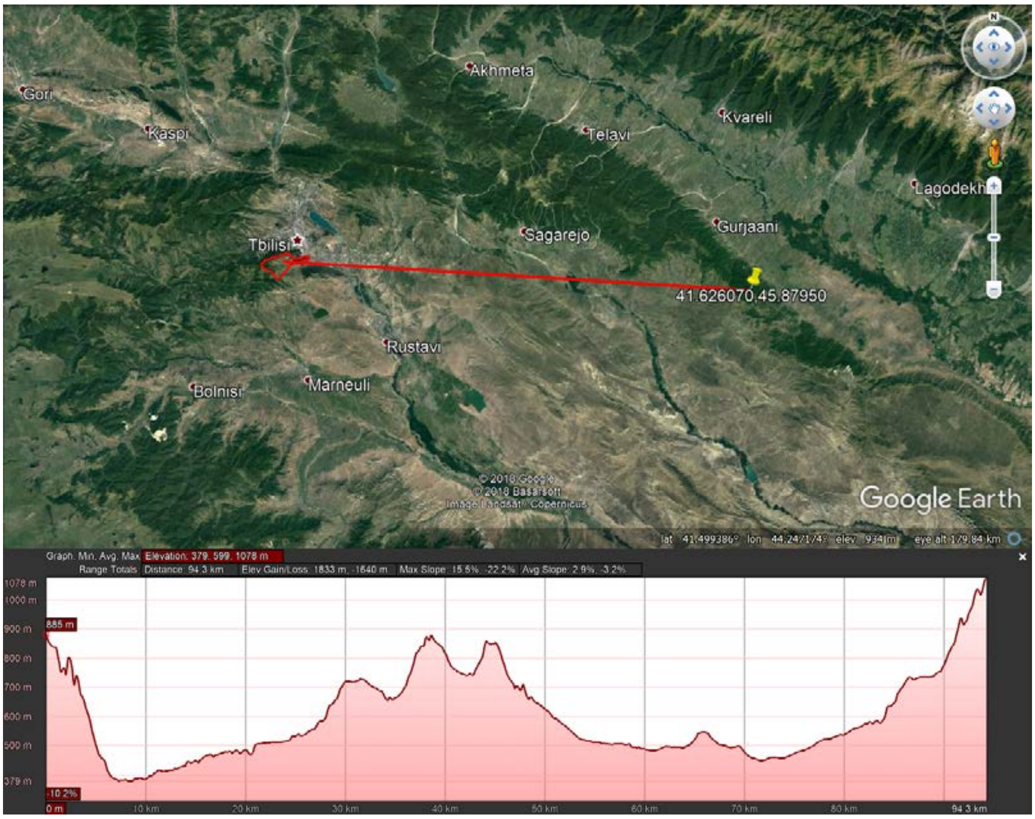

Figure 5 – Google Earth image showing the radar station location (yellow pin) and the Leghvtakhevi catchment (red polygon) including the elevation profile of the direct connection line (red line) where the radar station is located at the right end and the Leghvtakhevi catchment at the left end

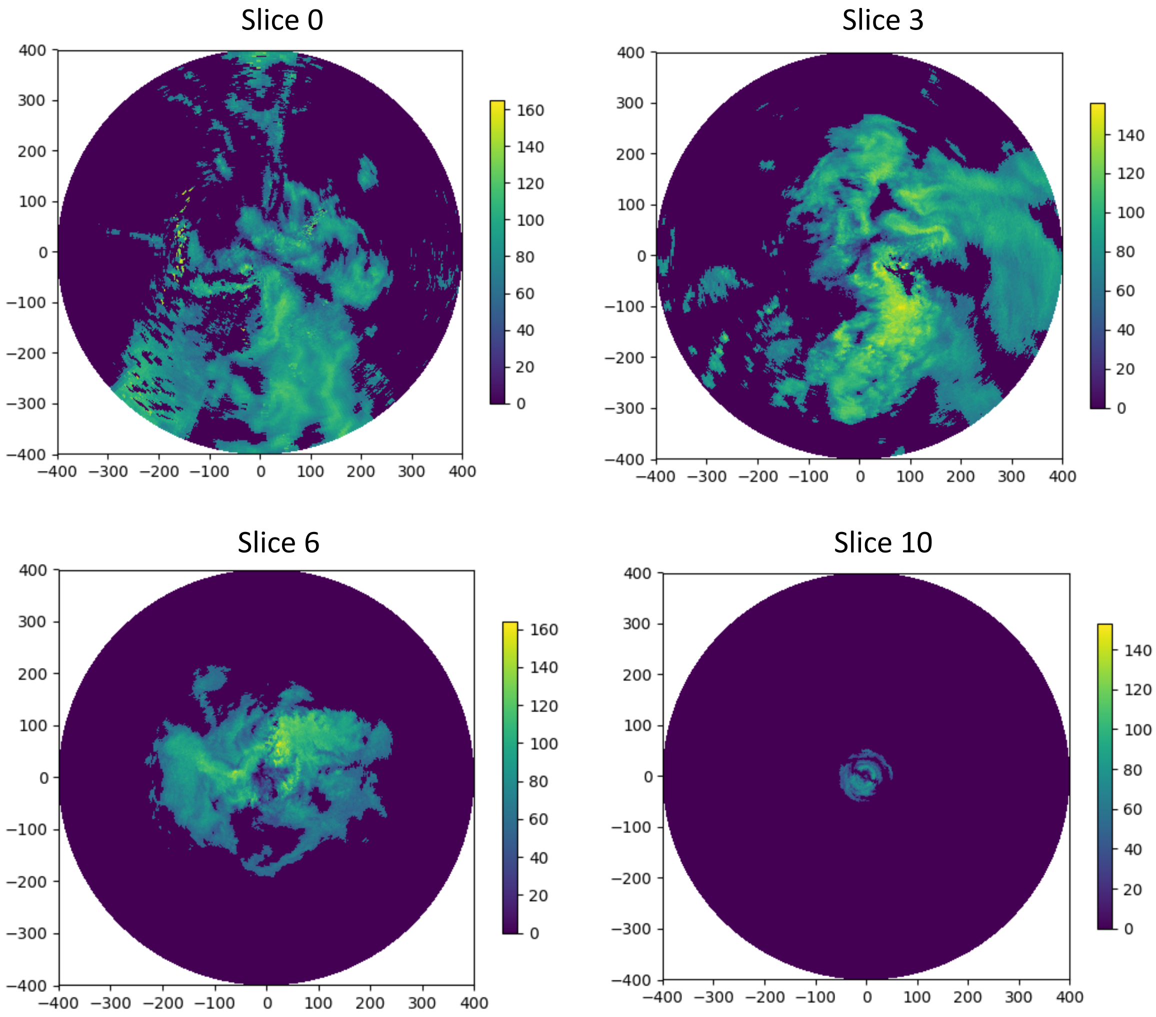

Figure 6 – Examples of radar reflectivity values (in dBZ) of different inclination slices for the rain event of the 23rd of September 2016; Note: The projection is rotated by -90°

(5) the radar observation points were converted to the WGS84 projection and the points located within the Leghtvakhevi catchment boundary (Figure 7) were summarized to obtain one precipitation estimate per 3min time interval.

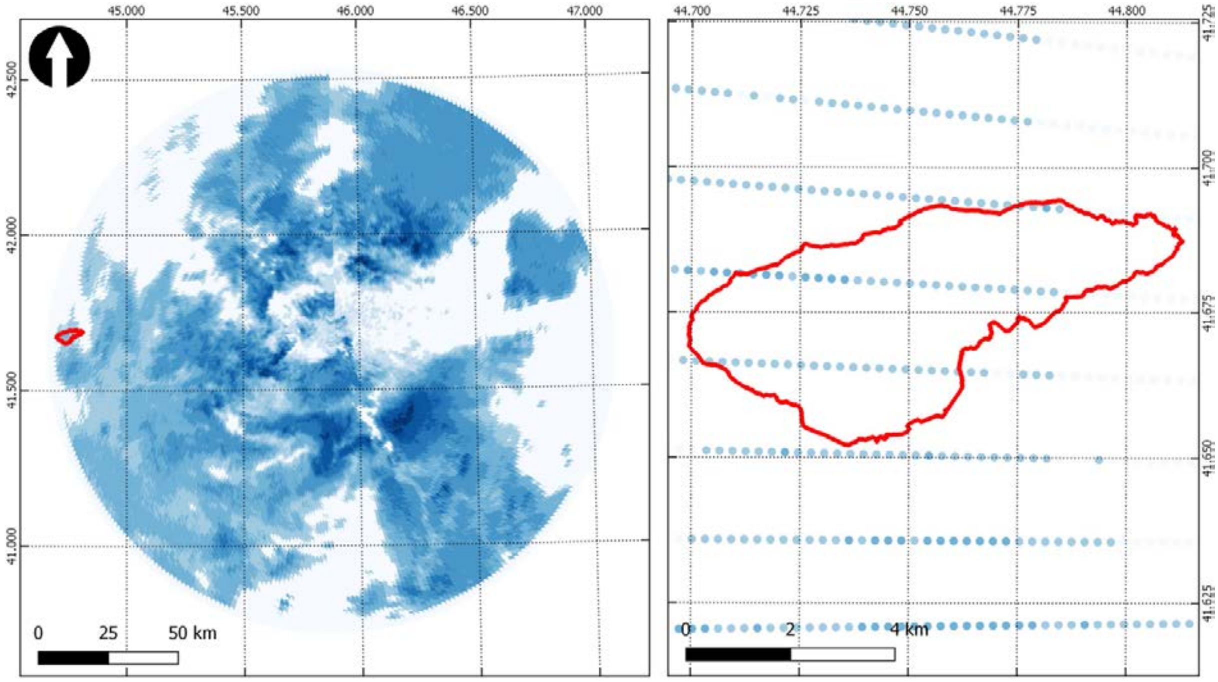

Figure 7 – Exemplary radar points projected to the WGS84 projection for the whole spatial data coverage (left) and for the Leghvtakhevi (right)

Using the described methodology, 3min rainfall time series were obtained for the different storm events. The comparison of the daily radar precipitation sums with ground observations shows a diverse picture (Table 4), ranging from good agreement to no agreement. This is not surprising, since the observations of the radar are almost 1000m above the ground in the Leghvtakhevi and since radar estimates should be calibrated on ground gages. In addition, it needs to be kept in mind that the Kojori data is spatially extrapolated, which is problematic especially for localized summer storms. The radar data will also not be used for predicting total rainfall depth. Instead, the time series obtained from the radar data is very valuable to disaggregate daily precipitation sums at Kojori to a sub-daily time step. In other words, each time series represents a possible option of how the daily precipitation sums observed at Kojori/Vashlijvari are distributed within shorter time-steps (Figure 8).

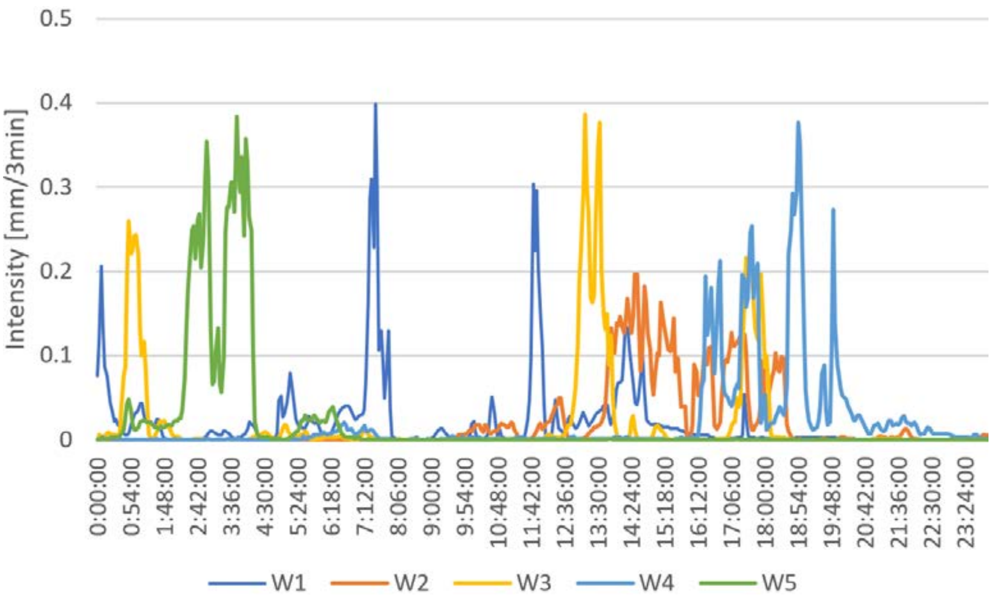

Figure 8 – Five radar data-derived time series of an arbitrary 10mm/d event (24hrs), disaggregated to 3-min time interval

3.5 Design storms for baseline and climate change

Extreme rainfall events (in mm/d) for baseline and climate change conditions are available from the Climate Change Report (Chapter 5.2) for 5, 25, 50, 100 and 500-year return periods (RP). Since no discharge observations in the Leghvtakhevi exist, the design storm RPs need to be directly translated to flood return periods.

Within the scope of this project, the five RPs will be evaluated for the baseline- and one climate change scenario. Therefore, the most conservative climate change projections were identified in close consultation with the Climate Change Expert. This is the RCP8.5 scenario for the time period 2070-2100, from which the precipitation for the five return periods was taken. According to the uncertainty ranges for each RP (boxplots in Figure 17) shown in the Climate Change report, we chose the median as being the most representative. This leads to the total design storm intensities as summarized in Table 5. Please note the significant differences between the baseline and climate change scenario. According to the projections, the current median of the RP500 will become the RP25 median.

Table 5 – Summary of total design storm precipitation rates for baseline and RCP8.5 climate change scenario for the period 2070-2090

Return Period	Precipitation [mm/d]	
	Baseline	Scenario RCP8.5 - 2070
RP5	66.95	167.86
RP25	105.96	199.91
RP50	124.89	204.98
RP100	145.02	208.95
RP500	199.91	212.94

The shown design storms represent total precipitation depth at one day (24 hrs). Due to the short response time of both the Vere and Leghvtakhevi, these values given in Table 5 need to be disaggregated to 3-min time series. It is obvious that distributing the precipitation evenly over all time steps would severely underestimate peak intensities. Therefore, the five different radar rainfall distributions (Figure 8) are scaled to the values given in Table 5. The sub-daily distributions of the RP5 to the RP500 are shown in the Annex (Figure 16).

3.6 Discharge data

Discharge data is not observed in the Leghvtakhevi River. The Vere catchment is the closest location where discharge is observed. In the Vere, daily discharge was observed from 1941 to end of 2014. Figure 9 shows the available discharge of the Vere and the processed precipitation data at Kojori.

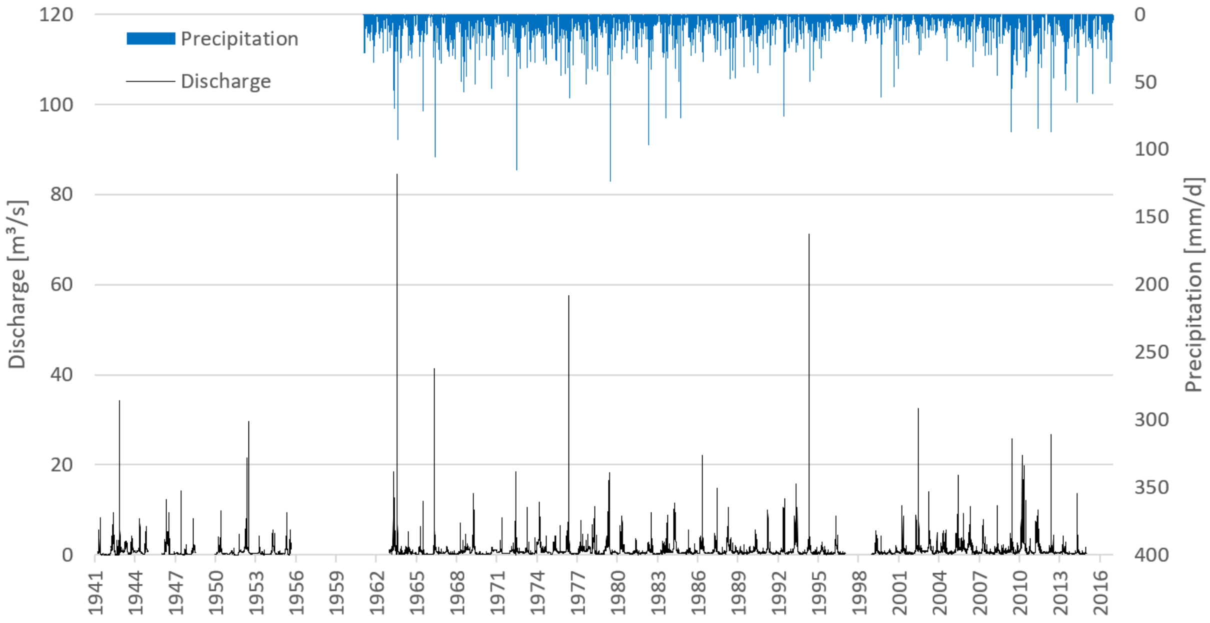

Figure 9 – Daily discharge in the Vere River and daily precipitation at Kojori

Unfortunately, the quality of the data is questionable: A hydrological report of the Georgian Department of Hydrometeorology mentions that in 1972, discharge in the Vere was 155.3m³/s, which is obviously not the case for the available data shown in Figure 9. In addition, the Vere hydrological report mentions discharge data in 1960 (July 04th with 259 m³/s), a time period where no data is available in the supplied records. The data should hence be handled with care and additional analysis were carried out: The correlation of the overlapping time period between discharge and precipitation is $r^2 = 0.11$. A possible impact of groundwater delay processes was tested by correlation analysis of lagged streamflow, but these correlations were lower. In addition, groundwater flow throughout the years is very low (around 0.2 m³/s) in the Vere. Calculating the correlation for May to September yielded a similar result ($r^2=0.13$), which shows that snow processes do not significantly impact hydrology. Therefore, it can be assumed that the hydrological response of the catchment is mainly governed by direct rainfall-runoff relationships.

3.7 Selection of calibration events

A calibration of the transformation and routing parameters which influence the shape of the hydrograph and the peak flows is unfortunately not possible using daily data from the Vere. The response time of 5.4 hrs of the Vere causes that peak flows cannot be resolved on a daily time step. Hence, averaged daily discharge data without knowing the maximum flood peak cannot be adequately used to calibrate parameters influencing the shape and peak of the hydrograph.

However, model parameters governing the flow volume (the area below the hydrograph) can be calibrated. Therefore, the three highest discharge events on record, August 1963, May 1976 and April 1994 were selected and will be used to calibrate loss parameters in HEC-HMS (Annex, Figure 17).

For the calibration of individual events, antecedent moisture conditions prior to the event are important to be included in the model. Therefore, antecedent conditions in terms of soil water deficit (in mm) for the three events has been calculated from the observed precipitation data and average monthly potential evapotranspiration (PET) using the Thornwaite method on available temperature data from Tbilisi airport. The moisture deficits amount to 15.2mm, 0mm and 13.4mm for the 1963, 1976 and 1994 event, respectively.

4 Methodology of hydrological modelling

HEC-HMS 4.2.1, developed by the U.S. Army Corps of Engineers, was chosen as the hydrological model after careful evaluation of options and close coordination with NEA. Main reasons were, that HEC-HMS is freely available, that it is a sophisticated and well-tested model for flood analysis dating back 30 years of development at the Hydrologic Engineering Center (HEC) and that it can be easily linked to the hydraulic model chosen for this study (HEC-RAS), sharing the same type of database (HEC-DSS).

HEC-HMS is capable to simulate both event-based and continuous simulations in time-steps from 1 minute to 1 day. The model has multiple algorithms for the individual hydrological processes from which the user has to choose the most appropriate ones for the particular simulation problem.

One HEC-HMS model is setup for the Leghvtakhevi and one for the Vere, utilizing the same data source and general setup process.

4.1 Model setup

Spatial data processing for HEC-HMS can be carried out using the software HEC-GeoHMS (here version 10.2 was used). Future versions of HEC-HMS will contain an own spatial data processing tool, making HEC-GeoHMS obsolete[5]. The setup process follows a structured process that is generally explained in the HEC-GeoHMS manual[6] and outlined for the Vere and Leghvtakhevi catchments in the following subchapters. In case of crashes or problems applying the software, guidelines and user groups can be screened for online support[7,8].

---

[5] http://www.hec.usace.army.mil/software/hec-geohms/downloads.aspx

[6] USACE. 2013. HEC-GeoHMS – Geospatial Hydrologic Modeling Extension. User’s Manual, Version 10.1

[7] http://www.hec.usace.army.mil/software/hec-geohms/known_issues.aspx

[8] https://community.esri.com/thread/43771

4.1.1 Pre-processing: Catchment delineation and project definition

Based on the DEM, the spatial delineation of the Leghvtakhevi and Vere catchment into sub-basins and streams is carried out. The workflow includes the processes: *DEM Reconditioning (Agree Method), Fill Sinks, Flow Direction, Flow Accumulation, Stream Definition* (threshold 200.000 cells = 0.2km² of the Flow Accumulation raster to initiate a stream)*, Stream Segmentation, Catchment Grid Delineation, Catchment Polygon Processing, Drainage Line Processing* and *Adjoined Catchment Processing*, where the output of one process provides input data for the subsequent ones. Due to the high-resolution DEM, computations of individual processes can take hours to complete.

The result of these process are delineated subbasins and streams that are the basis for the Project Setup. The project areas are spatially defined through the catchment outlets of the Leghvtakhevi and Vere.

4.1.2 Basin processing

In the Leghvtakhevi, the obtained spatial discretization must be furthermore refined to obtain subbasin outlets at the location of the linkage points to the hydraulic model. The linkage points represent the points where simulated discharges are transferred to the hydraulic model (Figure 3). Therefore, subbasins and streams need to be manually split and merged, from-and-to connections of the network schematic need to be set and identifier codes need to be adjusted and linked to the subbasins. Figure 10 shows the delineated catchment, where it can be seen that the spatial resolution is higher in the Leghvtakhevi due to the required links to the hydraulic model.

4.1.3 Characteristics of streams and subbasins

In the next step, subbasin and stream characteristics are derived from topographic information. This includes *Areas, River Length, River Slope, Basin Slope, Longest Flowpath, Basin Centroid, Centroid Elevation, Centroidal Longest Flowpath*. The derived data need to be manually checked for hydrologic consistency (e.g. river slope plausibility of positive downstream slopes) and the population of appropriate object ID values.

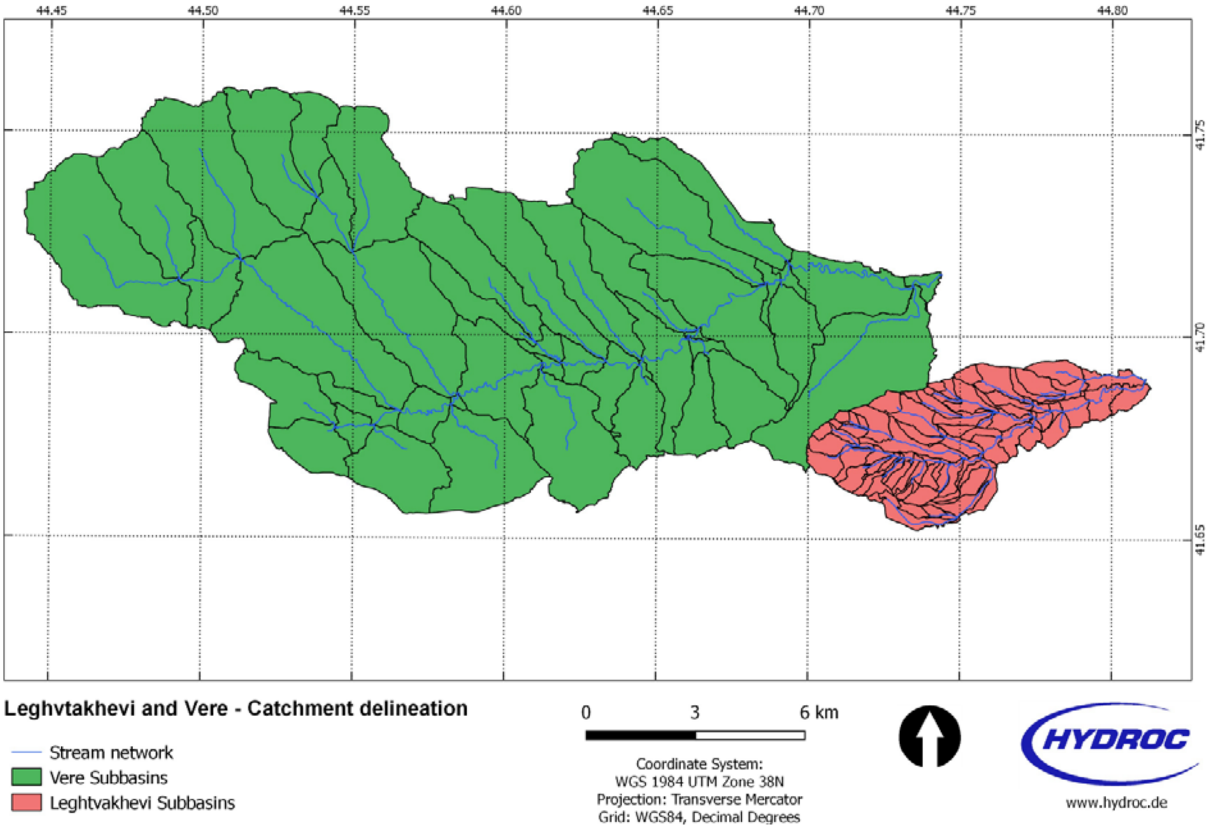

Figure 10 – Delineated stream network and subbasins of the Vere and Leghvtakhevi

4.1.4 Selection of algorithms

In this section, the appropriate algorithms have to be selected for the hydrological processes that will be simulated. Table 6 lists the available processes in HEC-HMS and the selected algorithms for the Leghvtakhevi and the Vere. In both catchments, the same algorithms are chosen that impact the generated flow volume for being able to transfer these parameters from the Vere to the Leghvtakhevi. The main difference between both setups lies in the *Transformation*- and *River Routing* methods. These are set to ‘None’ in the Vere since due to the lack of subdaily discharge data or observation of maximum peak flows, these parameters cannot be calibrated. For more detailed information about the individual methods and suggestions for selection of different calculation algorithms, please see the explanations in the following chapters and refer to USACE (2000)[14].

Table 6 – Depicted processes in HEC-HMS, chosen algorithms and model parameter settings

Process	**Selected algorithms Leghvtakhevi**	**Selected algorithms Vere**
Canopy storage	Simple Canopy with Simple Reduction	Simple Canopy with Simple Reduction
Surface depression storage	Simple Surface	Simple Surface
Infiltration (loss) method	Initial Constant Loss	Initial Constant Loss
Transformation method	Modified Clark	None
Baseflow	Constant Monthly	Constant Monthly
River Routing	Kinematic Wave	None
Channel losses/gain	None	None
Precipitation	Specified Hyetograph	Specified Hyetograph
Evapotranspiration	None	None
Snowmelt	None	None

4.1.5 Impervious areas, canopy- and surface depression storage

Canopy storage and surface depression storage cause initial losses at the onset of a storm event and depend on the vegetation type and surface properties of the catchment. Impervious areas cause a direct transformation of effective rainfall to runoff and do not induce constant losses during a storm. The areas are defined for each land use[9] and then averaged over each subbasin. These parameters are calculated for both the Vere and the Leghvtakhevi catchment.

---

[9] Maidment DR. 1993. Handbook of Hydrology. McGRAW-Hill Inc.

Table 7 – Land use characteristics impervious areas, canopy storage and surface storage

Land use	Impervious area ratio (%)	Canopy storage (mm)	Surface storage (mm)
Forest Light	0	2.5	1.0
Forest Dense	0	3.0	1.0
Water	100	0.0	0.0
Shrub Meadow	0	2.0	1.0
Shrub	0	1.5	1.0
Rocks	90	0.0	0.5
Urban High	60	0.0	0.2
Urban Low	40	0.0	0.5

4.1.6 Loss method parameter calculation

The loss method governs the surface runoff flow volume of the simulated storm event. In previous applications of HEC-HMS in the region, the *SCS-CN Loss Method* was applied[10]. It is a well-established, widely used and simple to apply method that has the advantage to incorporate both soil and land cover properties in the runoff formation. But it is not time-dependent, meaning that high intensity rainfall bursts are subject to the same losses per time step as low intensities, which causes underestimations of flows derived from intense rainfall events and makes the method unsuitable for this application. The *Initial and Constant Loss Method* uses an initial soil moisture deficit to calculate initial losses and Ks to calculate constant losses throughout the storm.

The initial estimation of Ks is based on the supplied soil- and land use data. Table 8 summarises the soil data available from the supplied soil maps. Hydrologic Soil Groups for the soils in the Leghvtakhevi have been derived from the Natural Resources Conservation Service Hydrology National Engineering Handbook[11], for the Vere, the groups were already available in the supplied data.

---

[10] HEC-HMS Models supplied by NEA

[11] United States Department of Agriculture, Natural Resources Conservation Service. 2007. Part 630 Hydrology, National Engineering Handbook, Chapter 7, Hydrologic Soil Groups.

Table 8 – Soil types, texture (available only for Leghvtakhevi) and Hydrologic Soil Group

Catchment	Soil Types / Texture	Hydrologic Soil Group
Leghvtakhevi	Brown forest soils, heavy loam and clayey	D
	Cinnamonic, heavy and medium loam	C or D
	Brown forest soil, weathering of sedimentary rocks.	C
	Meadow-field, heavy loam and clayey	D
	Cinnamonic, weakly developed, developed on loessial loams	C
	Cinnamonic, heavy and medium loam	C or D
Vere	Gray cinnamonic, Calcic Kastanozems	D
	Cinnamonic leached, Calcic Kastanozems	D
	Cinnamonic, Eutric Cambisols and Calcic Kastanozems	D
	Cinnamonic calcareous, Calcaric Cambisols and Calcic Kastanozems	C
	Brown forest, Eutric Cambisols	C

Since Ks varies with land use[12], the hydrologic soil groups are then overlaid by the reclassified land cover map and for each hydrologic soil group and land cover, Ks values are defined (Table 9), combining [11] and [12].

These values represent the initial Ks values of both catchments, which can be calibrated in the Vere- and then transferred to the Leghvtakhevi HEC-HMS model.

---

[12] Jariv N, Koestel J, Messing I, Moeys J, Lindahl A. 2013. Influence of soil, land use and climatic factors on the hydraulic conductivity of soil. Hydrol. Earth Syst. Sci. 17

Table 9 – Estimated saturated hydraulic conductivity (Ks) values for the soil and land cover combinations

Hydrologic Soil Group	Land Cover	Estimated saturated hydraulic conductivity (Ks) [mm/hr]
C or D	ForestLight	6
C or D	Shrub	4
C or D	ShrubMeadow	3
C or D	UrbanHigh	3
C or D	UrbanLow	3
C	ForestDense	12
C	ForestLight	10
C	Rocks	0
C	Shrub	8
C	ShrubMeadow	5
C	UrbanHigh	5
C	UrbanLow	5
C	Water	0
D	ForestDense	1.5
D	ForestLight	1.25
D	Rocks	0
D	Shrub	1
D	ShrubMeadow	0.5
D	UrbanHigh	0.5
D	UrbanLow	0.5

4.1.7 Transformation method parameter calculation

In the Leghvtakhevi, the translation of effective rainfall to the flood-wave is an important process for calculating peak flows. The *Clark Transformation Method* is well suited for application in the Leghvtakhevi since it is “particularly valuable for unusually shaped watersheds and for watersheds containing several physiographic areas such as plateaus, escarpments and valleys”[13]. Here, we are using the *Modified Clark Method*, which additionally discretises the catchment in grids to explicitly account for variations in travel time from all

---

[13] Sabol GV. 1988. Clark Unit Hydrograph and R-Parameter estimation. Journal of Hydraulic Engineering 114(1)

regions of a watershed[14]. The method calculates translation (movement) and attenuation (retention throughout the basin) of water based on two input parameters: the time of concentration (Tc) and a storage coefficient (R). Uncertainties in the calculation of Tc can be very high[15], mainly caused by different methods, design storms and resolution of topographic data. We tried to rule out most of these associated uncertainties by (1) utilising the full resolution of the 1m DEM without resampling the data to a coarser resolution, (2) taking the "TR-55" method which is based on physical watershed characteristics and calculates actual flow velocities, and (30) carrying out an analysis using the lowest (RP5) and highest (RP500cc) design storms to calculate Tc, which yielded a maximum difference of only 5% in Tc. The Tc was hence calculated for the RP100, which will cause a maximum uncertainty of 2.5% for the highest and lowest RPs. The influence of this uncertainty will be evaluated in the model's sensitivity analysis. An estimation of R is given by Sobol (1988)[13] with:

$$\frac{Tc}{R} = 1.46 - 0.0867 \cdot \frac{L^2}{A}$$

where Tc is the time of concentration, R is the storage coefficient, L is the longest flow path of the subbasin, and A is the subbasin area. Solving this equation for R, entering the area and flow length calculated from HEC-GeoHMS yields an estimation of R for each subbasin, which approaches Tc if the watershed is square ($L^2 = A$). Since Sobol (1988)[13] derived that equation empirically, it can lead to unrealistic R values (e.g. negative or very high) in case the subbasin is very unusually shaped. In cases where R<0, R was set to 0.5*Tc or in cases or R>1hr it was set to 2*Tc.

Finally, for the Modified Clark Method, the computationally demanding *Grid Cell Processing* needs to be carried out in HEC-GeoHMS.

---

[14] USACE. 2000. Hydrologic Modelling System HEC-HMS – Technical Reference Manual.

[15] Grimaldi S, Petroselli A, Tauro F, Porfiri M. 2012. Time of concentration: a paradox in modern hydrology. Hydrological Sciences Journal 57(2)

4.1.8 Routing method parameter calculation

Regarding the routing of the flood wave through the channel, the *Kinematic Wave Model* is best suited in the Leghvtakhevi because no data are available for calibration, flow is mostly confined in the channels and channel slopes are steep[14]. Parameters for the *Kinematic Wave Model* are distinguished between small tributary streams (river order 1 and 2) and the main Leghvtakhevi (higher river order 2). Approximate width has been read from Google Earth[16] (order 1+2: 1.5m, order 3+4: 4m), side slopes from the 1m DEM (order 1+2: 2, order 3+4: 1), Manning's n values were set based on experience using lookup tables[17] and photos from the river (order 1+2: 0.045, order 3+4: 0.04). The shape of all channels was set to Trapezoid.

4.1.9 HEC-GeoHMS model export and import in HEC-HMS

The final step in HEC-GeoHMS is the preparation of the input files for HEC-HMS. Data checks and the creation of all files that can be loaded to the HEC-HMS model (background maps, meteorological data files, …) are carried out. The generated *.basin* file can then be opened in HEC-HMS (here: Version 4.2.1). In case the import is not successful, the user can utilize older HEC-HMS versions and then import to the newest version. If individual parameter imports did not work, the user can manually add the parameters in the HEC-HMS user interface. Figure 11 shows the basin schematics of the Vere and Leghvtakhevi in HEC-HMS. Please note the area marked in red in Figure 11b, which probably drains via a culvert into the confluence of the Leghvtakhevi and the Kura, but does not directly contribute flow to the Leghvtakhevi River.

---

[16] Google Earth. 2017. V.7.3.1.4507, DigitalGlobe 2017.

[17] Chow VT. 1959. Open-Channel Hydraulics. The Blackburn Press.

(a)

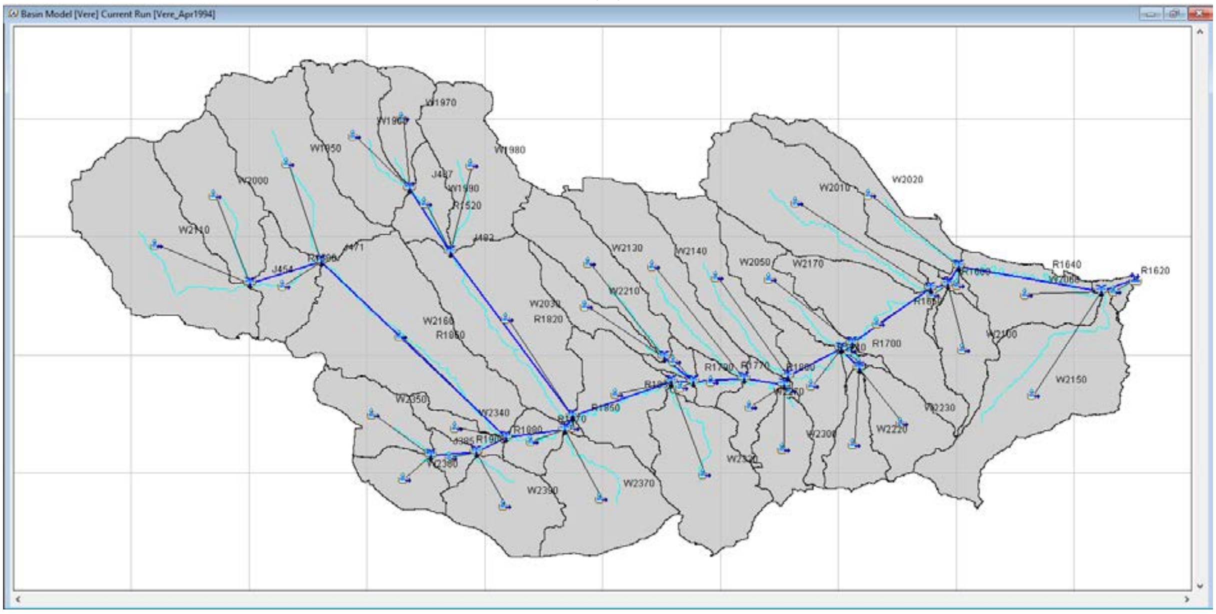

(b)

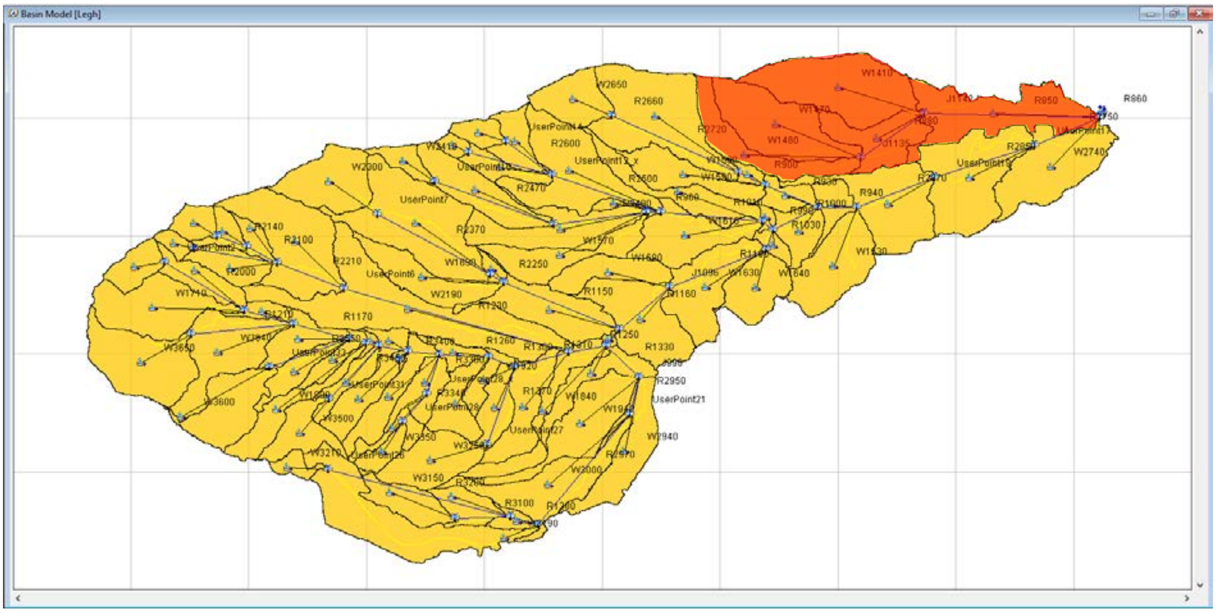

Figure 11 – HEC-HMS model schematics for the Vere (a) and Leghvtakhevi (b), area marked in red does not directly contribute flow to the Leghvtakhevi River

4.2 Model calibration in the Vere

Due to lack of appropriate data, as outlined in Chapter 3.6, a full calibration of the Leghvtakhevi model parameters regarding transformation and routing is not possible. However, based on the discharge data available in the Vere, an assessment of the simulated flow volumes for three selected calibration events (Chapter 3.7) was carried out. Therefore, the daily data of the three calibration events (Annex, Figure 17) was disaggregated to 3-minute time intervals using the five different radar sub-daily rainfall distribution options shown in Chapter 3.4, Figure 8). This step is essential because averaged daily rainfall intensities are lower than individual intensities of the 'true' distribution throughout 24 hours. Therefore, simulations are carried out in 3-minute time intervals and then aggregated to daily discharge volumes for being comparable to the daily average discharge observations in the Vere.

Table 10 summarizes the flow volumes for the three events (areas under the hydrographs). As can be seen, the different disaggregation options (W1-W5) cause significantly different flow volumes. Generally, the past events are more likely to be overestimated and the most recent event is more likely to be underestimated. This could be caused by multiple factors like (1) changes in the cross section at the discharge gauge over the years without adjusting the rating curve, (2) different rainfall and discharge observation devices / techniques or (3) changes in the catchment like intense land use change (deforestation, significant increase in urban areas) or (4) different sub-daily distribution of the rainfall, e.g. Aug-93 and May-76 event could have been caused by distribution W1, while Apr-94 event by W5 which would indicate a very good match of simulated to observed flow volumes (Table 10). Simulated vs observed hydrographs are supplied in the Annex, but it needs to be stressed that these simulations were carried out without transformation and routing options. We decided to calibrate Ks to the 1994-event for two reasons: First, it is the most recent event and resembles the current land use conditions best, and second, this will lead to a slightly more conservative model parameterization. Therefore, Ks values of the Vere model were adjusted until the simulation by distribution W5 of the Apr-94 event roughly matches the observations, which led to a decrease in Ks by 50%. The calibrated Ks values are still well within the physically plausible range for the soils present in both catchments. The same decrease was then transferred to the Leghvtakhevi model.

Groundwater contribution for the three events averaged about 2.5 m^3/s. These flows were distributed over the subbasins according to their catchment area, which leads to a groundwater contribution rate of 14.8 $L/s/km^2$. This value was then multiplied by the subbasin area and transferred for each month to the Leghvtakhevi model.

Table 10 – Observed and simulated flow volumes (Mill m^3) for the three selected calibration events in the Vere

Event	**Observed**	W1	W2	W3	W4	W5	**W5 Cal**
	Volume [Mill m^3]						
Aug-63	14.73	16.07	18.96	20.75	19.07	22.37	24.43
May-76	12.29	11.94	14.19	15.93	14.70	16.64	19.43
Apr-94	**15.43**	9.11	10.91	12.47	11.42	13.48	**15.16**

4.3 Sensitivity analysis of the Leghvtakhevi model

Calibration of the Leghvtakhevi model regarding timing and extent of peak flows is not possible due to lack of observed discharge data. Therefore, a sensitivity analysis was carried out to assess the uncertainty of the simulations. The Leghvtakhevi model simulations are carried out with the conservative assumption that the design events occur on saturated soils (antecedent moisture is assumed as “wet”). This does not include losses of the vegetation canopy and surface storages, which are assumed to occur. The 100-year RP was used as the event for which the sensitivities were evaluated at the outlet of the Leghvtakhevi, just upstream of the residential area. This analysis excludes the area circled in red in Figure 11b.

4.3.1 Sensitivity to different radar disaggregation events

The design storms shown in Figure 16 (Annex) for all radar disaggregation options (W1 – W5) were implemented in the above described model setup for the baseline RP100 event. The results show that option W5 leads to the highest peak flows, followed by option W3, W4, W1 and W2 (Figure 12). All shown events have the same total precipitation depth of 145 mm/d

(Table 5), the difference in the hydrographs ranging from 204 to 431 m³/s is only due to the temporal distribution of the rainfall intensities within the 24 hours simulation time. Since all distributions are possible to occur, we chose W5 for the further sensitivity analysis and for the predictions, since it is the most conservative option. When scaling sub-daily rainfall distributions to high return periods, it must be assessed if the resulting intensities are physically possible. W5 leads to maximum intensities of 8.17mm/3min and 66.97mm/30min for the RP500cc scenario, which have been observed in other places and are hence considered possible under future climate change[18].

Table 11 – Difference in peak flow due to the different sub-daily disaggregation options

	W1	W2	W3	W4	W5
Peak Flow [m³/s]	239	204	325	298	431

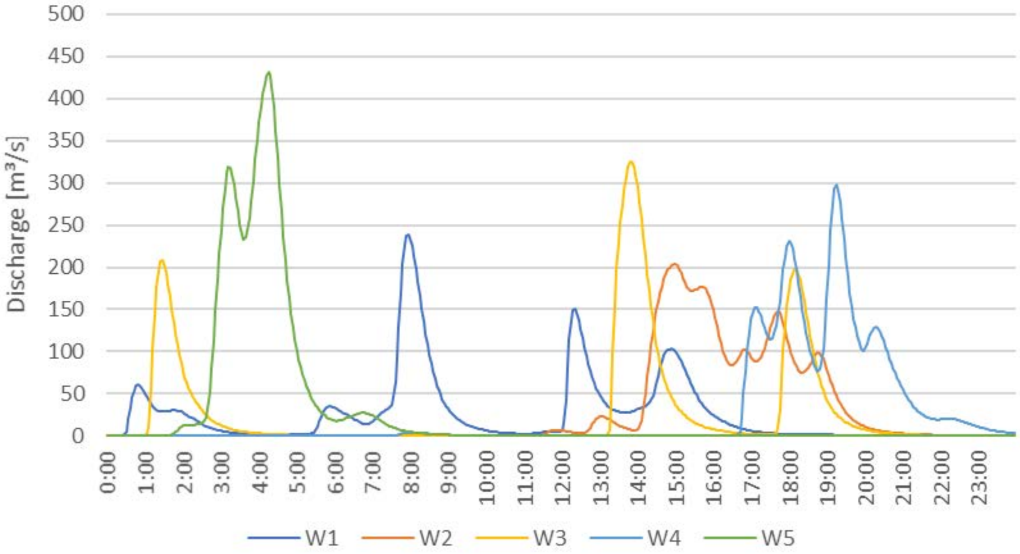

Figure 12 – Discharge simulations of the five different radar disaggregation options for the RP100 at the Leghvtakhevi outlet for the default setup with calibrated Ks values

---

[18] https://en.wikipedia.org/wiki/Rain#Wettest_known_locations

4.3.2 Sensitivity of the transformation parameters

Tc and R are linearly related since R is calculated from Tc with a linear equation. We therefore applied the sensitivity analysis modifying Tc by a reduction of 2.5% and increase of 2.5% as found during the calculation of Tc. In addition, we tested the sensitivity of a 50% reduction and increase by 100% (cut by half and double) to account for possible uncertainties that would arise when using a different Tc calculation method. The reduction in Tc leads to a quicker catchment response and higher peak flows, the increase in Tc to a slower catchment response and lower peak flows (Table 12, Figure 13). The impacts of the 2.5% variations are negligible, while the more extreme variations in Tc cause changes in peak flows of about ±10%.

Table 12 – Change in peak flow (in %) caused by the reduction and increase of Tc

	Tc*0.975	Tc*1.025	Tc*2	TC*0.5
Peak flow change [%]	0.4%	-0.5%	8.9%	-11.9%

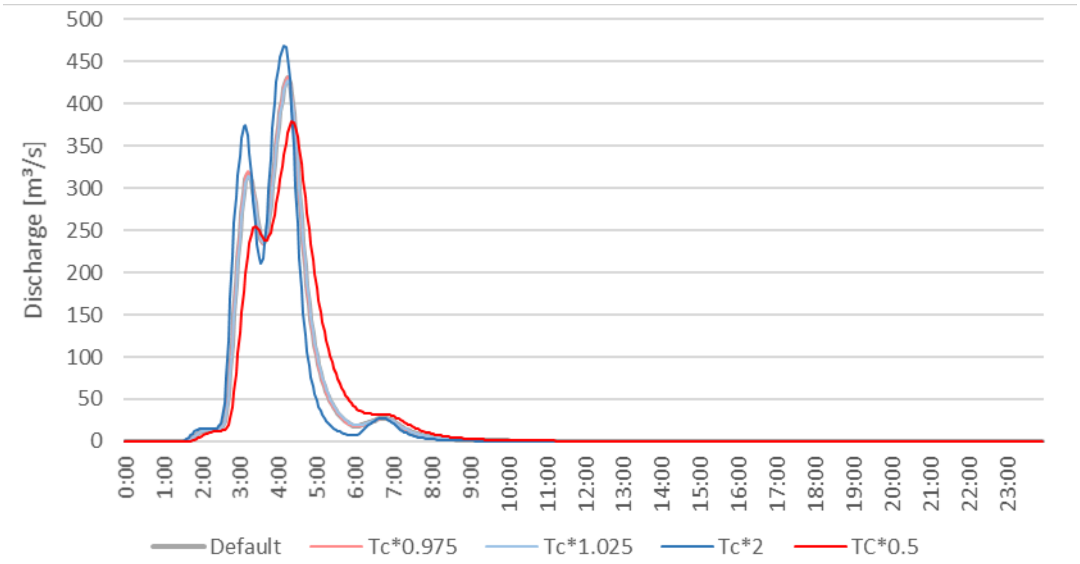

Figure 13 – Changes in discharge for the PR100 event for reduction (red) and increase (blue) in Tc

4.3.3 Sensitivity of the routing parameters

The Kinematic Wave Model uses the channel properties Length, Slope, Manning's n roughness value, Shape, Width and Side Slope to route the flood wave through the channels. Length and slope have been taken from the high-resolution DEM and are hence assumed to be sufficiently accurate. River Width and Side Slopes were varied by a reduction of 50% and increase by 100% (cut by half and double) which is considered to be within the uncertainty range of manually reading the values from the DEM and from satellite images. Manning's n values were varied between the usual range applied for natural streams of 0.03 and 0.05. The impacts of these parameter changes on the flood peak are negligible and different hydrographs cannot be distinguished. Therefore, the impacts are summarised in only.

Table 13 – Change in peak flow (in %) caused by the change in routing parameters

	Width times 0.5	Width times 2	Side Slope = 1	Side Slope = 4	Mannings n = 0.03	Mannings n = 0.05
Peak flow change [%]	-0.1%	0.0%	0.3%	-1.0%	0.7%	-0.4%

Results of the sensitivity analysis indicate that transformation and routing parameters can remain as is, without causing considerable uncertainties in the predictions. Hence, this model parameterization can be used for the simulation of the baseline- and climate change design storms. Therefore, the design storms as shown in Figure 16 (Annex) for the radar disaggregation "W5" are implemented in the model for all five return periods for the baseline and climate change scenario.

5 Results of hydrological modelling in the Leghvtakhevi

5.1 Baseline simulations

The results of the simulations for the baseline hydrographs are shown in Figure 14. It can be seen, that the individual RPs can be clearly distinguished and range between 189 m³/s for the RP5 to 601 m³/s for the RP500.

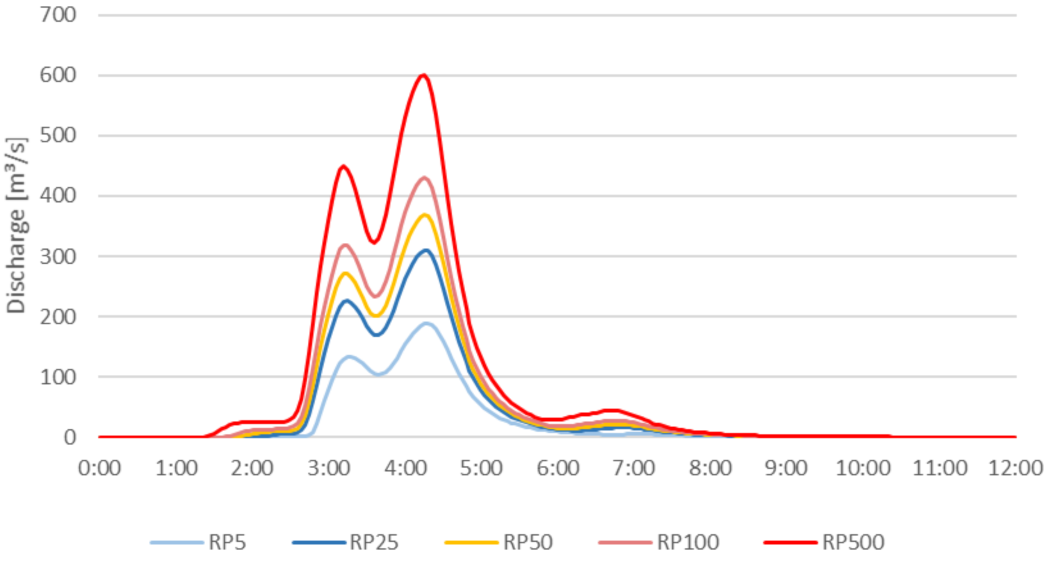

Figure 14 – Discharge hydrographs for the baseline return periods in the Leghvtakhevi

5.2 Climate change scenario simulations

As could be expected from the extreme change in precipitation (Table 5), the hydrographs under the RCP8.5 2070 climate change scenario (Figure 15) show a strong increase compared to the baseline. The most notable change occurs for the smaller RPs, while the RP500 is subject to the smallest increase. This causes that RP25, RP50, RP100 and RP500 are very close to each other under the climate change scenario.

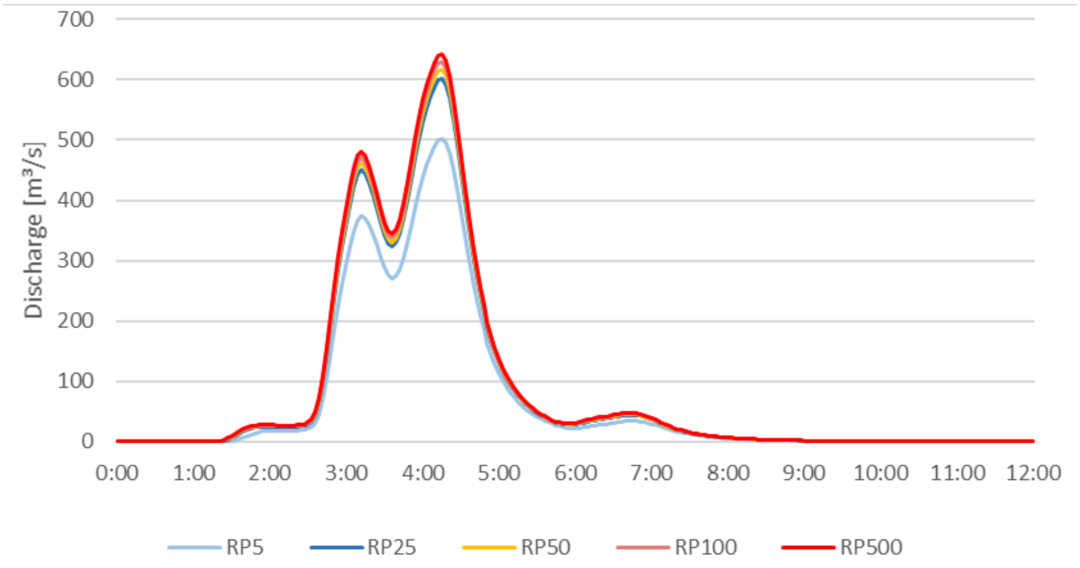

Figure 15 – Discharge hydrographs for the climate change scenario (RCP8.5, 20170) return periods in the Legthvakhevi

A direct comparison of the RPs and baseline vs. climate change peak flows is shown in Table 14, which confirms the visual interpretation of the hydrographs.

Table 14 – Comparison of baseline and climate change peak flows in the Leghvtakhevi

Peak flows [m³/s]	RP5	RP25	RP50	RP100	RP500
Baseline	189	310	369	431	601
RCP8.5 2070	502	601	617	629	642

5.3 Model coupling to HEC-RAS

All shown discharge hydrographs will be available for the baseline as well as climate change scenarios at all hydrological input locations to the hydraulic model. For the data transfer, each run is stored in a separate HEC-DSS file which has the same physical structure. HEC-RAS can be setup to read the discharges at all required points (Figure 3) for each scenario directly from the DSS-file. The shown hydrographs will then be transferred to inundation maps using HEC-RAS.

6 Discussion and conclusions

6.1 Key outcomes

The present hydrological modelling report presents, to our knowledge, the first estimation of flood discharges in the ungauged Leghvtakhevi catchment. The report shows the complete modelling process of data preparation, HEC-HMS model setup, model algorithm selection, parameterization, (restricted) parameter calibration, sensitivity analysis, and presentation of the model results. While this structure follows standard modelling applications, modelling efforts in the Leghvtakhevi were severely hindered by lack of crucial data which is required for simulating flood events, especially rare and extreme ones in fast reacting catchments as the Leghvtakhevi. Key outcomes of the report are therefore the methodological approaches to deal with these challenges:

A first valuable component of the report is the generation of the sub-hourly precipitation time series, using distribution mapping to extent the Kojori time series to enable an overlay with rainfall radar data to disaggregate the daily precipitation sums. Despite the fact that the method uses the best data available, major uncertainties stem from the lack of longer sub-daily time series which should include extreme rainfall events.

The second, and equally important point, concerns the lack of discharge observations in the Leghvtakhevi. Uncertainties in the rainfall input data and model parameters can be significantly reduced if reliable observations of discharge are available. To alleviate this problem, a second hydrological model, using the same data sources was setup in the neighbouring Vere catchment, where very basic calibration- and transfer of parameters to the Leghvtakhevi model was carried out. Again, care was taken to use all data sources to keep uncertainties originating from the ungauged catchment to a minimum.

The third key component of the report is the careful evaluation of the default parameters and the analysis of their sensitivity on the discharge simulation. This enables an assessment of the uncertainties involved in the model parameterization.

Finally, the study gives an estimation of design discharges under current and future conditions from RP5 to the extreme RP500. Results show, that current design events are subject to a wide spread in peak discharges. This spread is projected to decrease due to a more significant increase in the low RPs than the high RPs. Nevertheless, the discharges of all RP events are increasing from the baseline to the evaluated climate change scenario (RCP8.5, 2070).

6.2 Key assumptions, limitations and related uncertainties

Hydrologic modelling is always subject to a simplification of the naturally occurring processes. This simplification in both space and time introduces uncertainties in the simulations. These uncertainties can be minimized by selecting appropriate algorithms for the depiction of the processes as well as through choosing physically meaningful parameter values during the calibration process. We have carefully selected the most appropriate algorithms for the prevailing characteristics of the catchment and the task at hand. Therefore, the most important aspect in minimizing uncertainties in the simulations, is suitable precipitation and discharge data. Unfortunately, both data types are not available in the Leghvtakhevi catchment so that extrapolation, temporal downscaling and regionalization approaches needed to be used. These approaches inevitably introduce uncertainties into the predictions, which can, to a certain extent, be quantified through multiple simulations with modified input data (sensitivity analysis).

The sensitivity analysis showed that major uncertainties arise from the selection of the precipitation disaggregation option. The radar events used to derive the disaggregation time series represent only a small sample of the prevailing discharge patterns in the region. Due to lack of data, all evaluated options must be considered as equally likely and hence, the most conservative option was chosen here. This indicates, that an overestimation of the simulated discharges based on the design storms is more likely than an underestimation.

The derivation of design storms under current and future climate change conditions is also subject to considerable uncertainties, as outlined in the climate change report. Because only one set of baseline and one set of climate change RPs can be simulated in the whole model cascade, the simulations were limited to the medians of the design storms, which are considered as the most likely prediction.

Also, the parameter transfer of the loss method from the Vere to the Leghvtakhevi causes uncertainties. We have therefore evaluated discharge volumes for three flood events with different antecedent moisture conditions and for all available sub-daily rainfall distributions. The selection of the most recent flood as the governing event for the calibration was also the most conservative selection. This indicates that the calibrated loss parameters are more likely to cause an overestimation of surface runoff than an underestimation.

In comparison to all the above, the sensitivity analysis showed that minor uncertainties arise from parameter estimates regarding the effective rainfall transformation and flood routing.

In summary, it must be noted that despite the extensive effort made to reduce uncertainties in the predictions, the shown results should be seen as first estimates of design floods in the Leghvtakhevi. These should be adjusted through follow-up studies once a more suitable and reliable database is compiled.

6.3 Recommendations

The following recommendations are given to obtain an appropriate database for enhancing the reliability of flood modelling in the region:

- Installation of sub-hourly and long-term, gage-based precipitation observations to obtain a higher certainty in total storm intensity and in the sub-hourly distribution of rainfall events
- Installation of sub-hourly and long-term water level and discharge observations for being able to carry out a comprehensive calibration and validation of all sensitive and uncertain input data and model parameters
- A longer overlapping time period of radar data and gauged rainfall data should be obtained to obtain more reliable disaggregation time series
- In addition, a simple and cost-effective way to observe is the recording of information about how often and when certain paths in the Leghvtakhevi gorge are unpassable or when, where and under which conditions pedestrian infrastructure becomes damaged

As shown in recent history, the region is subject to extreme flooding. According to our analysis, this is expected to increase under climate change. The establishment of a flood forecast and early warning system could give threatened locations and residents' valuable lead- and preparation time. However, due to the fast response times of the catchments, a reliable weather forecast, including real-time processing of radar data, is the most important component in such a system. If a hydrological model is used within this system, continuous simulations need to be carried out to reliably track soil moisture conditions over time.

7 Capacity Building and Dissemination

The training program with theoretical background information, presentations, software and data packages for the hands-on practical training is currently prepared for the 10-day course to be held in Tbilisi after coordination and agreeing on a suitable time period with the Client. Emphasis during the training will lie on model conceptualization, data sources and -input, comparing model simulations and understanding uncertainties.

A key component of the capacity building and dissemination workshop will be the handing-over of the developed models, which can be used on Windows-based computers.

8 Annex

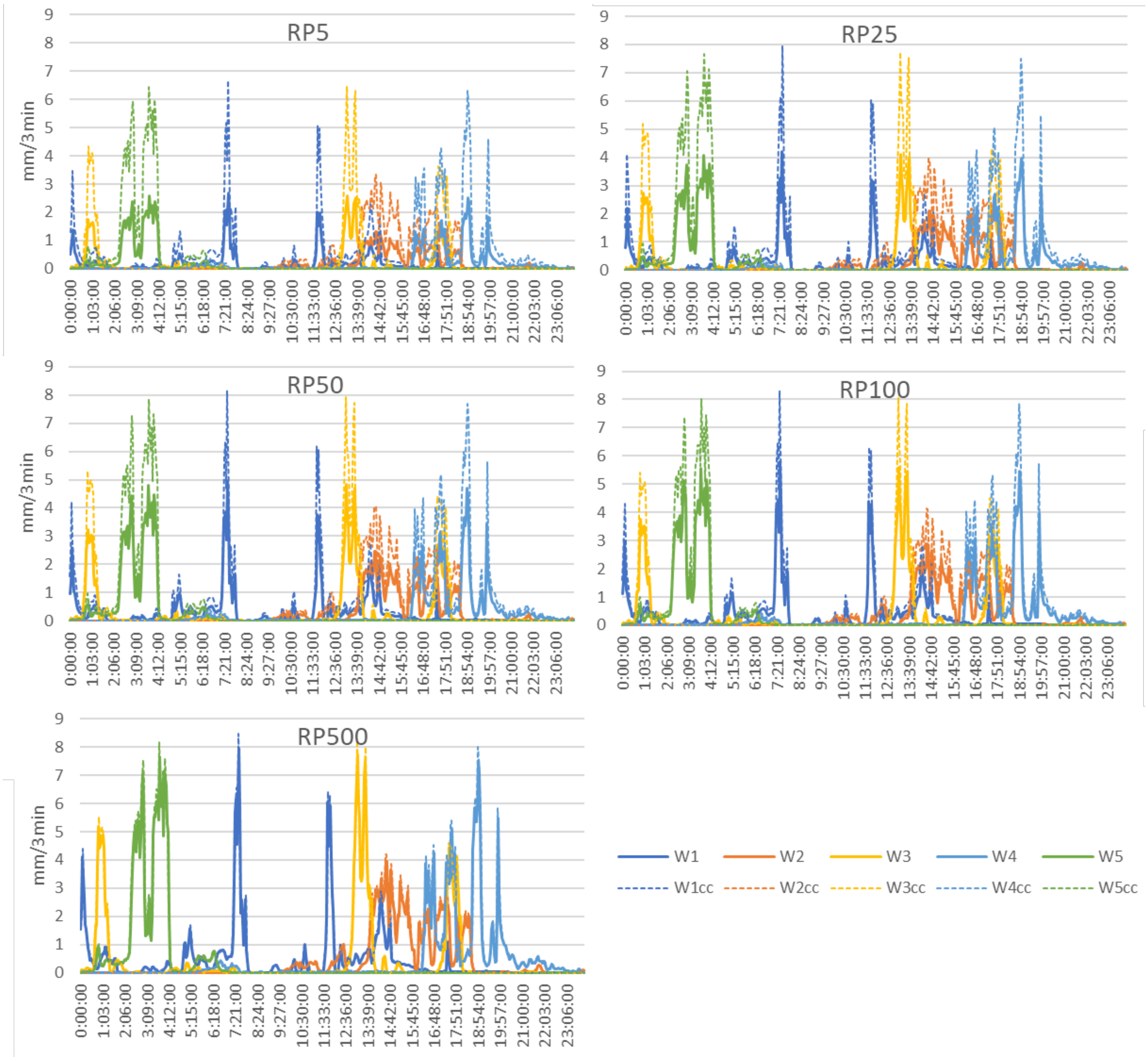

Figure 16 – Disaggregated design storm events in 3-min time step (mm/3min) for RP to RP500 for the baseline (W1 – W5) and climate change scenario (RCP8.5, 2070-2090, W1cc – W5cc)

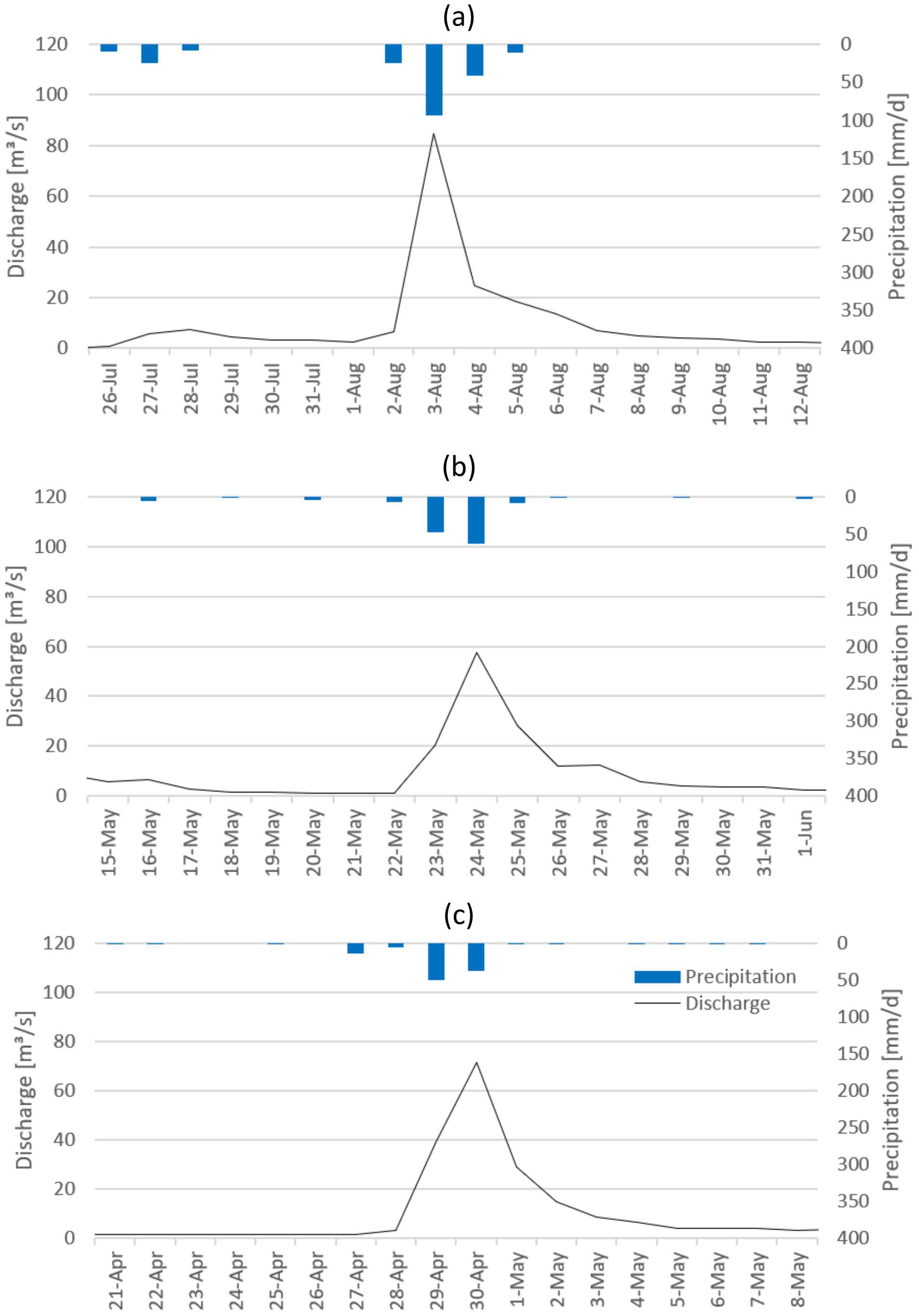

Figure 17 – Precipitation and discharge for the three calibration events in the Vere: (a) August 1963, (b) May 1976 and (c) April 1994.

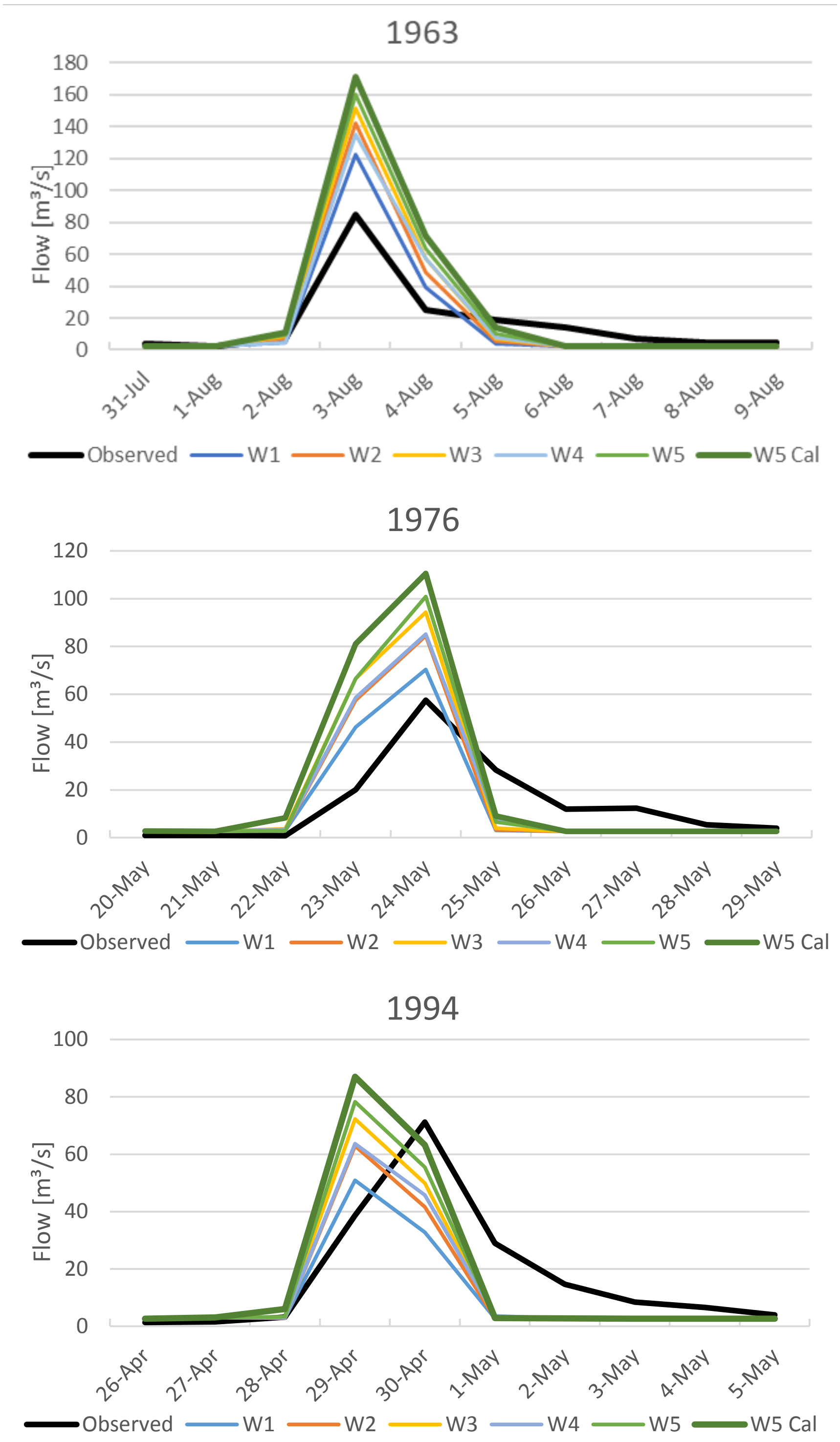

Figure 18 – Comparison of simulated and observed hydrographs using the different sub-daily disaggregation options for the three calibration events (Figure 17)